Desalination and Water Treatment
www.deswater.com
doi: 10.1080/19443994.2014.926840

55 (2015) 1609–1619
July

Taylor & Francis
Taylor & Francis Group

Adsorption kinetic and isotherm of methylene blue, safranin T and rhodamine B onto electrospun ethylenediamine-grafted-polyacrylonitrile nanofibers membrane

Sajjad Haider[a,*], Faez F. Binagag[a], Adnan Haider[b], Asif Mahmood[a], Nasrullah Shah[c], Waheed A. Al-Masry[a], Salah Ud-Din Khan[d], Shahid Mahmood Ramay[a]

[a]*Department of Chemical Engineering, College of Engineering, King Saud University, P.O. BOX 800, Riyadh 11421, KSA, Saudi Arabia, emails: shaider@ksu.edu.sa, afridi_phd@hotmail.com (S. Haider), ajjaj_f@hotmail.com (F.F. Binagag), ahayat@ksu.edu.sa (A. Mahmood), walmasry@ksu.edu.sa (W.A. Al-Masry), smramay@yahoo.com (S.M. Ramay)*
[b]*Polymer Science and Engineering Department, Kyungpook National University, #1370 Sankyuk-dong, Buk-gu, Daegu 702-701, South Korea, email: adnan_afridi9294@yahoo.com*
[c]*Department of Chemistry, Abdul Wali Khan University, Mardan, Pakistan, email: nasrchem@hotmail.com*
[d]*Sustainable Energy Technologies Center, King Saud University, P.O. BOX 800, Riyadh 11421, Saudi Arabia, email: drskhan@ksu.edu.sa*

Received 12 February 2014; Accepted 16 May 2014

ABSTRACT

EDA-g-PAN NFs membrane was prepared via electrospinning and chemical grafting techniques. Grafting (64%) with no change in the physical nature and colour was confirmed by FT-IR spectra. Adsorption kinetics of methylene blue (MB), rhodamine B (RB) and safranin T (ST) dyes onto PAN and EDA-g-PAN NFs membranes showed equilibrium time of around ~60 min. The adsorption kinetic followed pseudo-second-order model and intraparticle diffusion was not the only rate-limiting step. The adsorption data for the dyes fitted well to Langmuir and Freundlich equations. The order of adsorption capacity (q_{max}) obtained from Langmuir plot was: MB (94.07 mg/g) < ST (110.62 mg/g) < RB (138.69 mg/g). These values are more than most of the values reported in literature.

Keywords: Nanofibers (NFs); Ethylenediamine (EDA); Adsorption kinetics; Dyes

1. Introduction

The shift in societies toward industrialization is considered to be the hallway toward development. Industries, such as mining, metallurgical, tannery, chemical manufacturing and processing, textile, printing, paper and plastic, etc., play a very critical role in the economic development of any society. The bulk of the raw materials used in these industries come from organic and inorganic origins. The discharge of by-products from these industries into fresh water, without taking proper safety measure, in the form of heavy metal ions and dyestuff could cause contamination [1]. The toxic effects of heavy metals and dyestuff on human health, aquatic flora and aquatic micro-organisms have been under intense investigation worldwide. Heavy metal ions are documented to cause various diseases such as dehydration, stomach ache, nausea, dizziness and/or lack of coordination in muscles, destruction of the

*Corresponding author.

nervous systems of young children, lung irritation, eye irritation, skin rashes, vomiting, abdominal pain, lung insufficiency, liver damage, etc. [2]. Whereas dyestuff are aesthetically distressing, prevent re-oxygenation in water by shielding the penetration of sunlight, toxic to aquatic micro-organisms and is even carcinogenic to humans in some cases [3].

Thus, the removal of dyestuff from wastewaters has received increased attention [4–14]. Hence, beside conventional materials (such as peat, red mud, coir pith, neem leaf, activated sludge, waste organic peel, tree fern and minerals, adsorbents, etc.) and techniques (chemical precipitation, reverse osmosis, electro-deposition, ion exchange, evaporations oxidation process, electrochemical reduction, etc.), new adsorbents and technologies have also been explored [15]. Amongst the mentioned methods adsorption is considered to be a cheaper, simple, attractive and favourable alternative for the removal of dyestuff from wastewater [4–14,16]. Taking into account the advantages (i.e. easy functionalization and the high surface to length ratio) of nanomaterial, their preparation and their application in the wastewaters treatment are recently immensely focused. Among these materials electrospun nanofibers with fibre diameter in the range of 10–500 nm, high porosity, high-gas permeability, and high-specific surface area per unit mass have attracted enormous attention. It has been reported that adsorbents with the functional groups such as carboxyl, sulphonic and phosphonic favour metal ions and dyes adsorption through the ion-exchange mechanism, while those containing nitrogen facilitate metal ions adsorption through chelation and dyes through hydrogen bonding mechanisms [17–22].

Polyacrylonitrile (PAN), due to its binding ability, is frequently used as an active component of ion-exchangers. PAN based polymer has the advantage of relatively easy modification of its physico-chemical properties (e.g. hydrophilicity, porosity, mechanical strength, etc.). This distinctive property is imparted to PAN by the presence of nitrile group. PAN forms hydrogen bonds, and donor–acceptor complexes (chelation) with positively charged species [23].

In our continuous efforts, in the present study, we have combined electrospinning technique with chemical grafting. PAN was electrospun to fabricate NFs (with an average diameter of 225 nm) membrane. The NFs were then surface grafted with EDA in a simple chemical reaction and were applied to the removal of the cationic dyes from synthetic waste waters. No work with EDA grafting of NFs for the removal of dyes from wastewater has been reported.

2. Materials and methods

2.1. Materials

PAN (molecular weight (Mw) 150,000), N,N-dimethylformamide (DMF (C_3H_7NO)), EDA ($C_2H_8N_2$·2HCl), MB ($C_{16}H_{18}ClN_3S$·$3H_2O$), RB ($C_{28}H_{31}Cl$·N_2O_3) and ST ($C_{20}H_{19}Cl$·N_4) were purchased from Sigma-Aldrich. All the chemicals were used without further purification. The solutions for dyes were prepared in distilled water.

2.2. NFs membrane/sheet

A 10 wt. % PAN solution was prepared by dissolving 1 g of PAN into 10 mL DMF. The solution was stirred on a magnetic stirrer at 25˚C for 24 h to obtain homogeneous PAN solution. The prepared PAN solution was then added to a 5 mL plastic syringe and was electrospun using optimized electrospinning parameters. After electrospinning the solution for 1 week (~6 h daily), the NFs sheets/membranes were dried in the vacuum oven at 50˚C and −0.1 MPa and stored for further characterizations.

2.2.1. Morphology of the NFs

The PAN NFs created via electrospinning at optimized electrospinning parameters were studied using a FE-SEM (JSM-7600F). NFs samples were fixed onto a holder with aid of a carbon tape and then placed in the sputtering machine for platinum coating to increase their electrical conductivity. After platinum coating the morphology of electrospun NFs was examined via FE-SEM.

2.2.2. NFs diameter measurement

The average diameter of the NFs was measured by randomly selecting 100 fibres from the FE-SEM micrograph of each sample. The diameters were measured using adobe photoshop software program. The measurements were then converted to actual value using the scale bar on the FE-SEM micrograph. The histograms of the NFs diameters were plotted using sigma plot software program.

2.3. EDA grafting

The reaction of EDA with PAN nitrile group is shown in Fig. 1. EDA-g-PAN was prepared by immersing PAN NFs in a 1.66 mol L^{-1} EDA solution in 250-mL beaker and sealed. The mixture was heated and stirred on a water bath at 90–95˚C for different

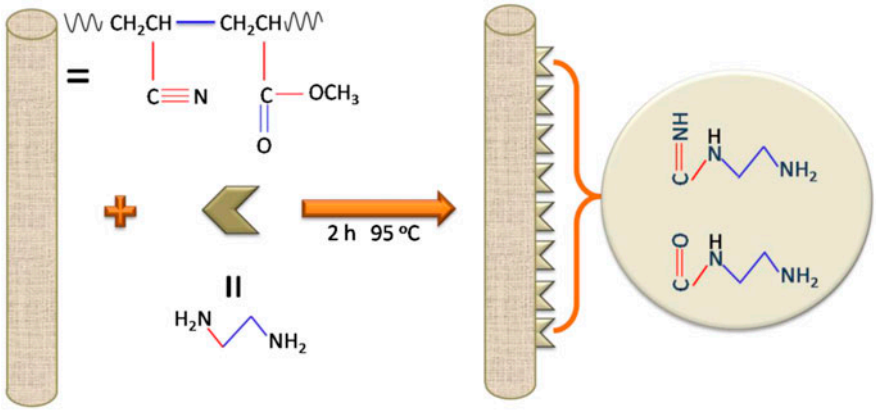

Fig. 1. Grafting EDA to PAN NFs.

time durations (1, 2, 3 and 4 h). After the reaction, the mixture was cooled to 25°C. NFs membranes were washed several times with distilled water and acetone, dried at 60°C in an oven and stored for characterization. The percentage grafting was calculated according to Eq. (1):

$$C_n = \frac{W_1 - W_0}{W_0}\frac{M_0}{M_1} \times 100 \quad (1)$$

where C_n is % grafting of PAN to EDA-g-PAN, W_0 is the weight of the PAN NFs membrane before reaction, W_1 is the weight of the PAN NFs membrane after reaction, M_1 and M_0 are the Mws of EDA (60.10 g/mol) and Acrylonitrile (AN) monomer (53.06 g/mol), respectively [24].

2.4. FT-IR analysis

Infrared spectra of the PAN and EDA-g-PAN NFs membranes were studied using FT-IR spectrometer (Bruker Vertex 70). The potassium bromide (KBr) discs of the samples were prepared by mixing and grounding the membranes samples with KBr powder in mortar with a pestle. The mixture was then shaped into discs under hydraulic press. The samples discs were placed into the sample compartment of the FT-IR and spectral measurements were recorded in the wave number range of 400–4,000 cm^{-1}. The data were baseline corrected and normalized in origin 6.1 and plotted in sigma plot.

2.5. Adsorption

Dried samples of PAN and EDA-g-PAN membranes were separately added to 10 mL of 400 ppm synthetic solutions of dyes (MB, RB and ST (Fig. 2)) and shaked (in a shaker bath) by a batch technique as a function of time until 240 min at 25°C. Equilibrium time was determined from the saturation point of the adsorption kinetics data. Adsorption equilibrium isotherm was studied at 25°C as a function of the concentrations of the dyes. The concentrations of dyes in solution after adsorption experiment were determined with UV/VIS spectrometer (Perkin Elmer, Lambda 35). The amount adsorbed was calculated using the following formula:

$$q = \frac{(C_0 - C_f)\,V}{M} \quad (2)$$

where q is the amount adsorbed (mg g^{-1}), C_0 and C_f are the initial and final concentrations (mg L^{-1}), respectively, for dyes, V is the solution volume (L) and M is the amount of adsorbent (g) used.

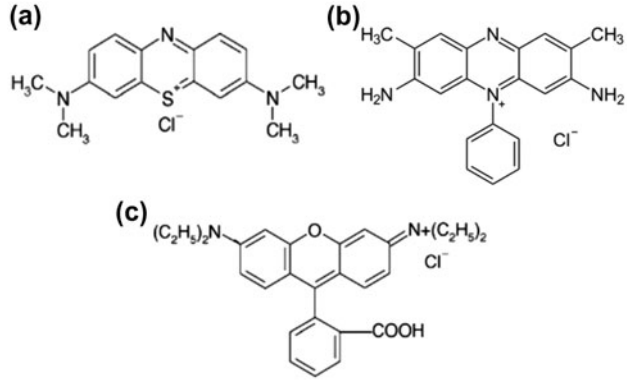

Fig. 2. Structures of cationic dyes; (a) MB, (b) ST and (c) RB.

3. Results and discussion

3.1. EDA grafting and morphology

Table 1 shows the data for the grafting of EDA to PAN. The percentage grafting of EDA increased as the time was increased. The maximum grafting 64% was observed at 2 h. This increase in the grafting of EDA is attributed to the faster and increased molecular diffusion of EDA from the solution into the NFs membrane until a critical saturation time. Further increase in the time led to decrease in the EDA grafting. The physical nature of EDA-g-PAN NFs membrane

Table 1
EDA grafting to PAN NFs membrane

Exp. no	Time (h)	Temp. (°C)	Conversion %	Colour	Softness
1	1	90–95	6.713779	White	Soft
2	2		64.74321	White	Soft
3	3		38.78682	White	Soft
4	4		34.444766	White	Soft

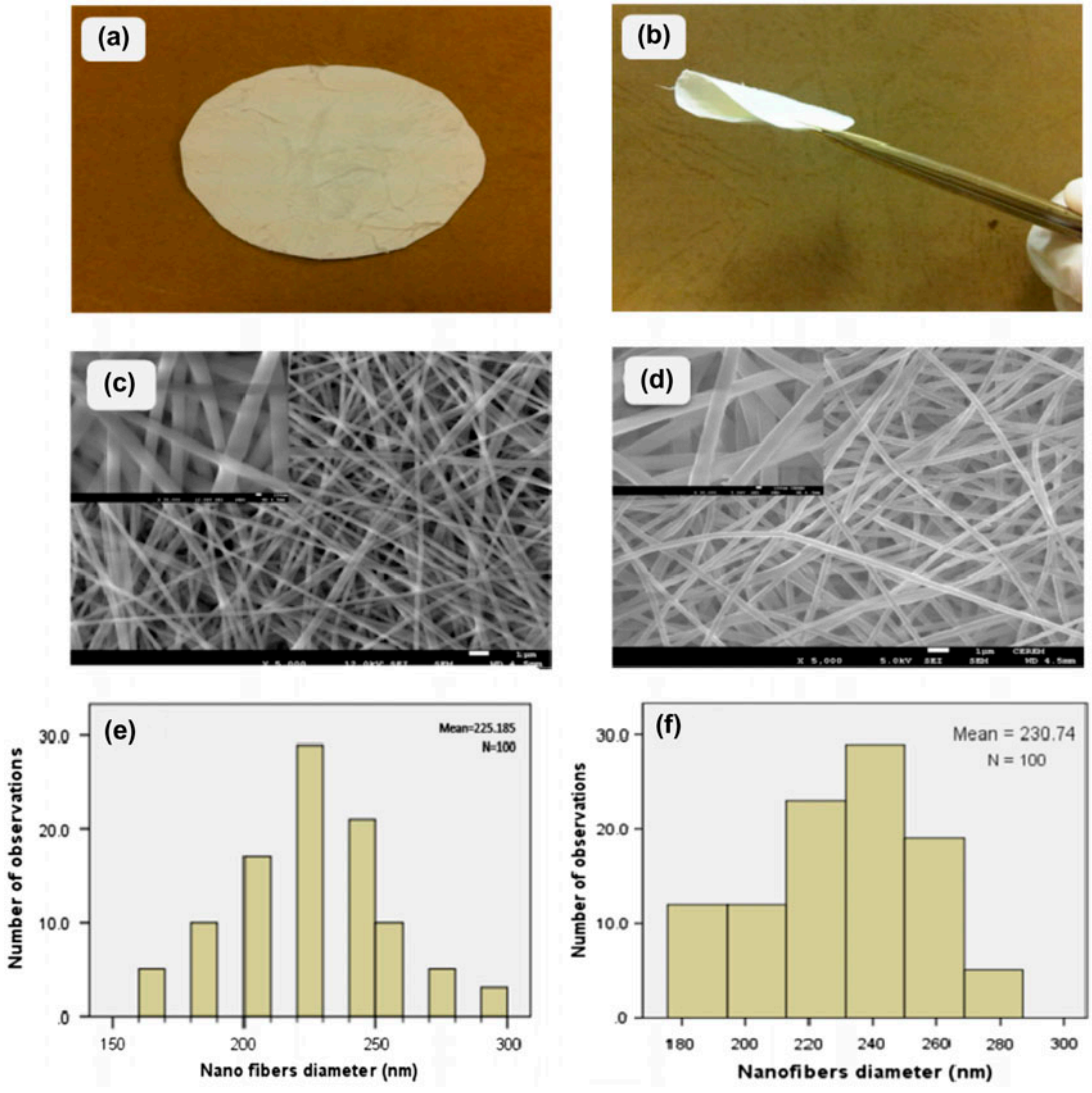

Fig. 3. Digital images of; (a) PAN and (b) EDA-g-PAN (the sample is soft). FE-SEM micrographs of the surface; (c) PAN, (d) EDA-g-PAN and histograms of the diameter; (e) PAN and (f) EDA-g-PAN.

remained white and soft in all the experiments. Fig. 3(a)–(f) shows the digital images, FE-SEM micrographs and the histograms for the diameter of PAN and EDA-g-PAN NFs membranes. The digital images for the EDA-g-PAN NFs membrane showed soft physical texture (Fig. 3(a) and (b)), which shows that the grafting of EDA did not affect the physical texture of the NFs. The micrographs of EDA-g-PAN NFs membranes exhibited similar surface morphology to that of the PAN membrane without deterioration and degradation (Fig. 3(c) and (d)). This result further complement our arguments in favour of the unchanged physical texture of PAN NFs. The average diameter of the PAN NFs is, however, only slightly increased from 225 to 230 nm (Fig. 3(e) and (f)), which is attributed to the chemical grafting of EDA to PAN NFs.

3.2. FT-IR study

Fig. 4 shows the FT-IR spectra of PAN and EDA-g-PAN NFs membranes at various reaction times. PAN exhibited the characteristic bands in region of 1,000–1,300 cm^{-1} (C–O stretching), at 1,453 cm^{-1} (CH_2 bending), 1,700 cm^{-1} (C=O stretching), 2,241 cm^{-1} (C≡N stretching) and 2,938 cm^{-1} (CH stretching). The presence of C–O and C=O stretching bands in the spectra of the PAN, suggests that PAN is a copolymer of acrylonitrile and methylacrylate [25,26]. All the characteristic bands of PAN were observed in spectrum of EDA-g-PAN. The intensity of the sharp band at 2,241 cm^{-1} continuously decreased until its intensity decreased to maximum around 2 h, whereas the band at 1,700 cm^{-1} is not only decreased but also shift to the lower frequency. The conversion at 2 h was 64% (Table 1) and the NFs membrane was soft. Besides,

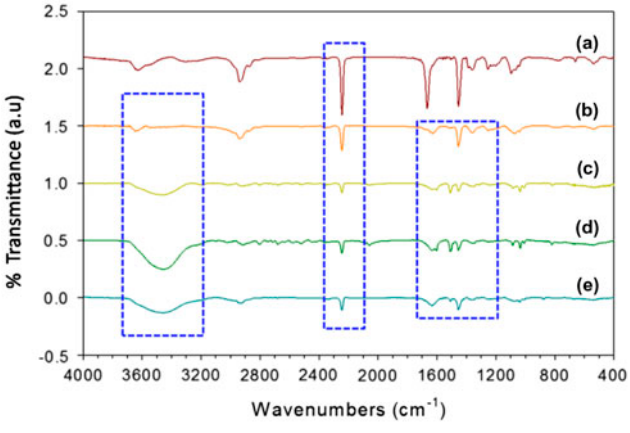

Fig. 4. FT-IR spectra of (a) PAN NFs and EDA-g-PAN NFs membranes at different reaction time: (b) 1, (c) 2, (d) 3 and (e) 4 h.

decreased intensities of the old, some new bands, whose intensities increased continuously with increase in the reaction time, were also observed. For example, the intensities of the broad band in regions of 3,300–3,550 cm^{-1} (N–H stretching) and 1,630–1,670 cm^{-1} ([C=N], and some traces of amide [C=O stretching vibration] were increased. Furthermore, two new bands in the region of 1,450–1,480 cm^{-1} (CH_2 and N–H bending) were also observed [27,28]. The data presented in the FT-IR clearly shows that EDA is grafted to PAN. The reduced broad band in the region of 1,630–1,670 cm^{-1} could also be attributed to the formation of hydroxamic acid [29].

3.3. Adsorption kinetic

Fig. 5(a) and (b) illustrates the adsorption kinetic of MB, RB and ST onto the PAN and EDA-g-PAN NFs membranes from 100 ppm synthetic solution. The shapes of the adsorption curves for all the three dyes suggest that the binding of dyes to the active sites onto the adsorbent increased sharp until 30 min and level off around ~60 min (Fig. 5(a)). This suggests that equilibrium between adsorption and desorption of dyes is achieved i.e. the surface is homogeneously saturated. The adsorption capacity of PAN and EDA-g-PAN NFs membranes for dyes increased in the order PAN < EDA-g-PAN (Fig. 5(b)). The increased dyes adsorption for EDA-g-PAN NFs membranes is credited to the improved number of active sites onto the membranes with grafting. Furthermore, RB illustrated superior affinity (MB < ST < RB) onto PAN and EDA-g-PAN NFs membranes (Fig. 5(a) and (b)).

To understand the destiny of the dyes molecules adsorbed onto PAN and EDA-g-PAN NFs membranes, the kinetic data were analyzed by pseudo-first-order (Eq. (3)) and pseudo-second-order kinetic (Eq. (4)) models. Pseudo-first-order kinetic model is based on the assumption that the adsorption rate is related to the unoccupied adsorptive sites and only one adsorbate can adsorb onto one adsorptive site on the adsorbent surface. Whereas, pseudo-second-order kinetic model assume that adsorption should relate to the squared product of the difference between the number of the equilibrium adsorptive sites onto an adsorbent and that of the occupied sites i.e. one adsorbate is adsorbed onto two sorption sites on the surface [30].

$$\log(q_{1e} - q_t) = \log(q_{1e}) - \frac{K_1}{2.303}t \quad (3)$$

q_{1e} and K_1 can be obtained by the intercept and slope of plot of log $(q_{1e} - q_t)$ vs. t.

$$\frac{t}{q_t} = \frac{1}{K_2 q_{2e}^2} + \frac{1}{q_{2e}} t \quad (4)$$

q_{2e} and K_2 can be obtained by the slope and intercept of plot of t/q_t vs. t.

Fig. 6(a)–(d) and Table 2 show that the kinetic data fitted best to pseudo-second-order kinetic model

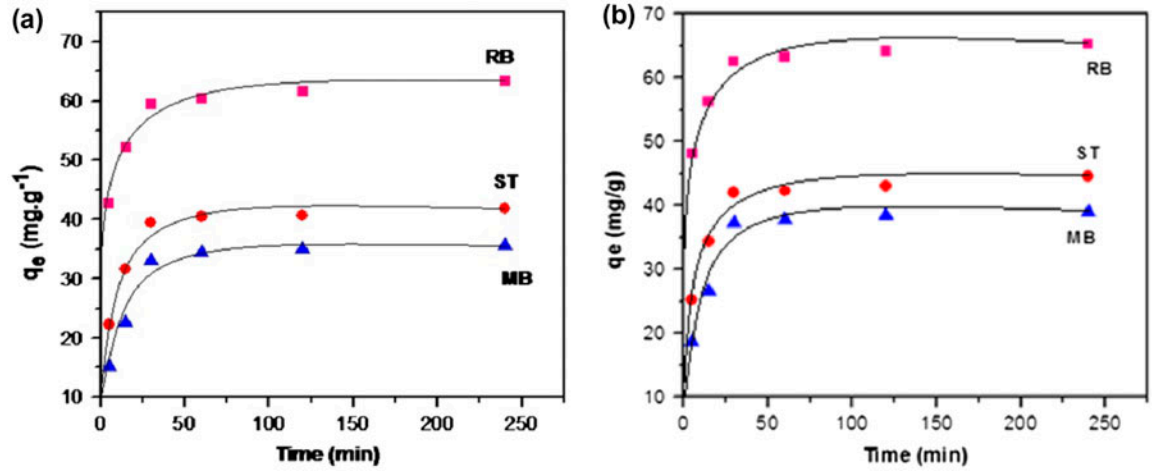

Fig. 5. Adsorption kinetics of dyes onto NFs membranes; (a) PAN and (b) EDA-g-PAN.

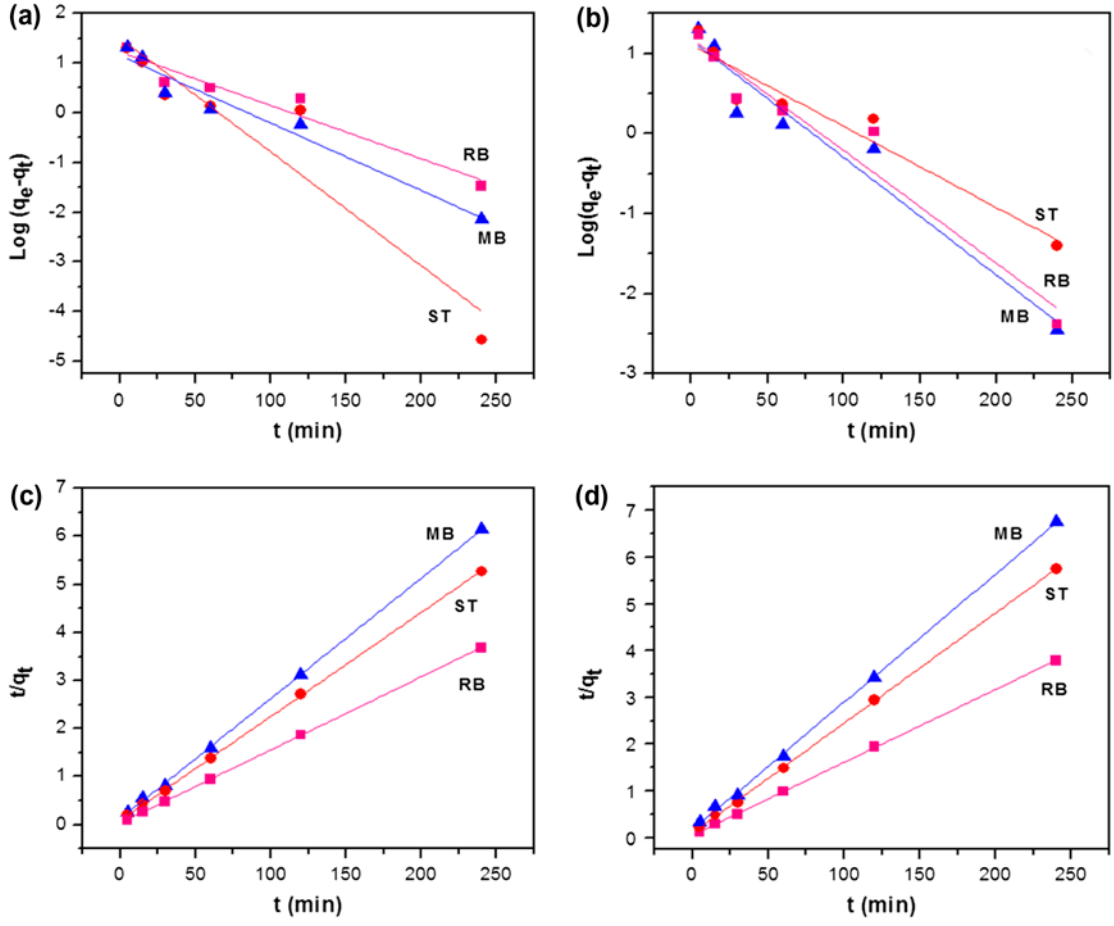

Fig. 6. Pseudo-first-order; (a) PAN and (b) EDA-g-PAN, and pseudo-second-order; (c) PAN and (d) EDA-g-PAN.

Table 2
Calculated and experimental "q" values for the pseudo-first and second-order kinetics models

Dye	Adsorbent	q_{exp}	Pseudo-first-order			Pseudo-second-order		
			K_1	q_{1e}	r^2	K_2	q_{2e}	r^2
MB	PAN	35.523	0.031	14.178	0.946	0.0046	36.523	0.999
	EDA-g-PAN	39.037	0.034	14.665	0.931	0.0052	39.904	0.999
RB	PAN	63.467	0.025	16.679	0.935	0.0049	64.062	0.999
	EDA-g-PAN	65.1956	0.032	15.545	0.935	0.007	65.703	0.999
ST	PAN	41.800	0.053	32.06	0.879	0.006	42.463	0.999
	EDA-g-PAN	45.561	0.023	12.644	0.911	0.0055	46.168	0.999

(correlation coefficient [r^2] 0.999 (Fig. 6(c) and (d))) compared to pseudo-first-order kinetic model (r^2 varied from 0.879 to 0.946 (Fig. 6(a) and (b))) [31]. Alongside good fitting, the q_{2e} values calculated from the pseudo-second-order kinetic model for the adsorbed dyes were much closer to the experimentally q_{exp} values (Table 2). These results suggested that the adsorption of dyes molecules onto on the surface of NFs membrane followed pseudo-second-order kinetic model.

A typical liquid/solid adsorption generally involves film diffusion, intraparticle diffusion and mass action. Since for physical adsorption, mass action is a very swift process, hence for kinetic study it could be neglected. Adsorption kinetic is usually controlled by liquid film diffusion or intraparticle diffusion i.e. rate-limiting step is either liquid film diffusion or intraparticle diffusion [32]. Therefore, adsorption diffusion models are mainly constructed to describe the process of film diffusion and/or intraparticle diffusion. In a batch adsorption system, the prospect of diffusion was studied by the intraparticle diffusion model (Eq. (5)) [33]. This model assume that the plots of q_t vs. $t^{1/5}$ should yield a straight line through the origin when the intraparticle diffusion is the only rate-controlling step of the adsorption kinetics [34,35].

$$q_t = K_d t^{1/2} \tag{5}$$

where k_d is the diffusion coefficient value, t is the time and q_t is the amount of dye adsorbed.

Fig. 7(a) and (b) shows non-linear plots of q_t vs. $t^{1/2}$ for dyes. Deviation from validity test indicates that intraparticle transport is not the only rate-limiting step. The plot of the whole range of time is divided into three distinct regions. The first sharp region shows adsorption whereas in the second region, beside adsorption, diffusion may also occur. Diffusion in the second region could attribute to diffusion between the layers of a fibre. The third region represents the equilibrium; here due to saturation intraparticle diffusion starts to slow down [36].

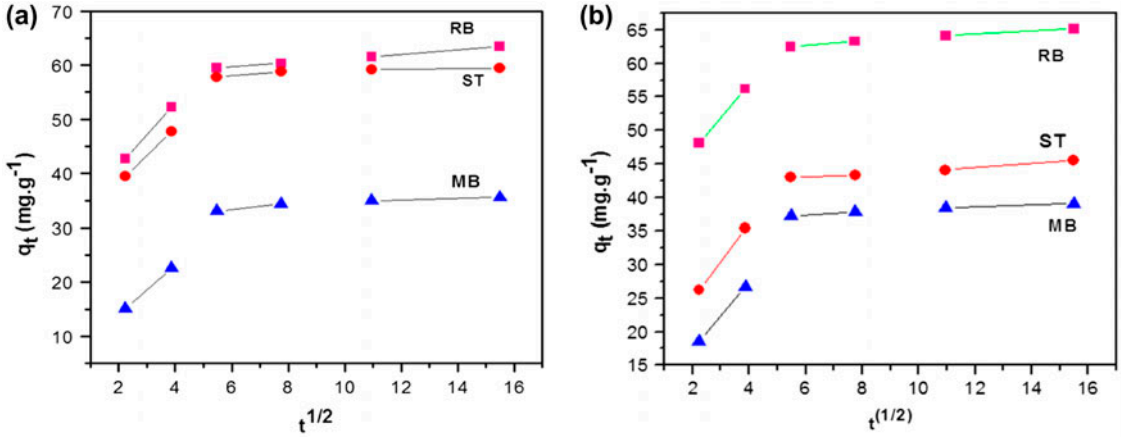

Fig. 7. Intraparticle diffusion plots; (a) PAN and (b) EDA-g-PAN.

3.4. Equilibrium adsorption

Fig. 8(a) and (b) shows the adsorption of dyes onto the PAN and EDA-g-PAN NFs membranes as a function of concentration (C_e). Adsorption showed rapid increase initially, however, as the concentrations of the dyes solution is increased, adsorption is gradually decreased. To understand the phenomenon of the adsorption onto the PAN and EDA-g-PAN NFs membranes, the equilibrium adsorption data were applied to Langmuir and Freundlich isotherm models [37].

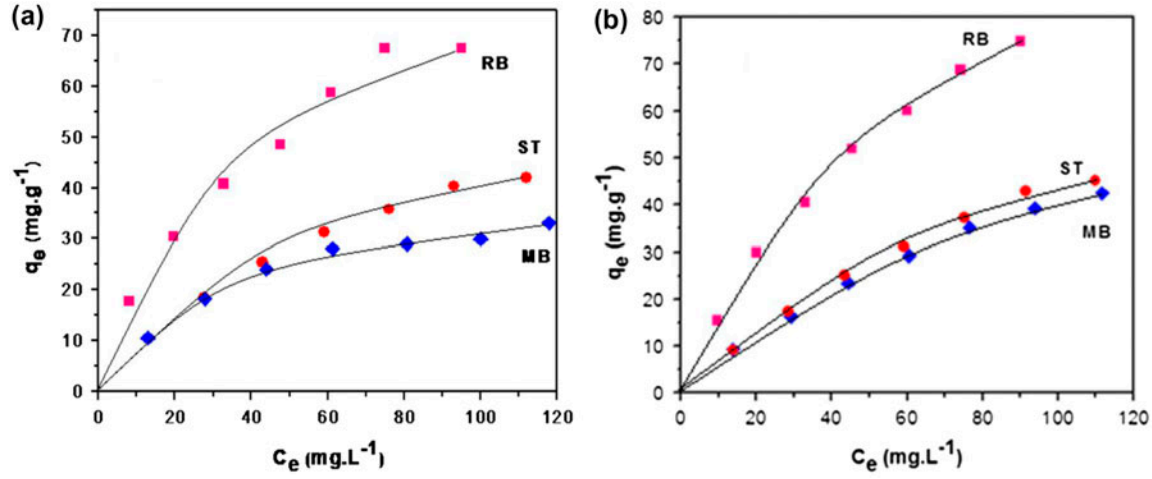

Fig. 8. Adsorption isotherms of dyes on to; (a) PAN and (b) EDA-g-PAN NFs membranes.

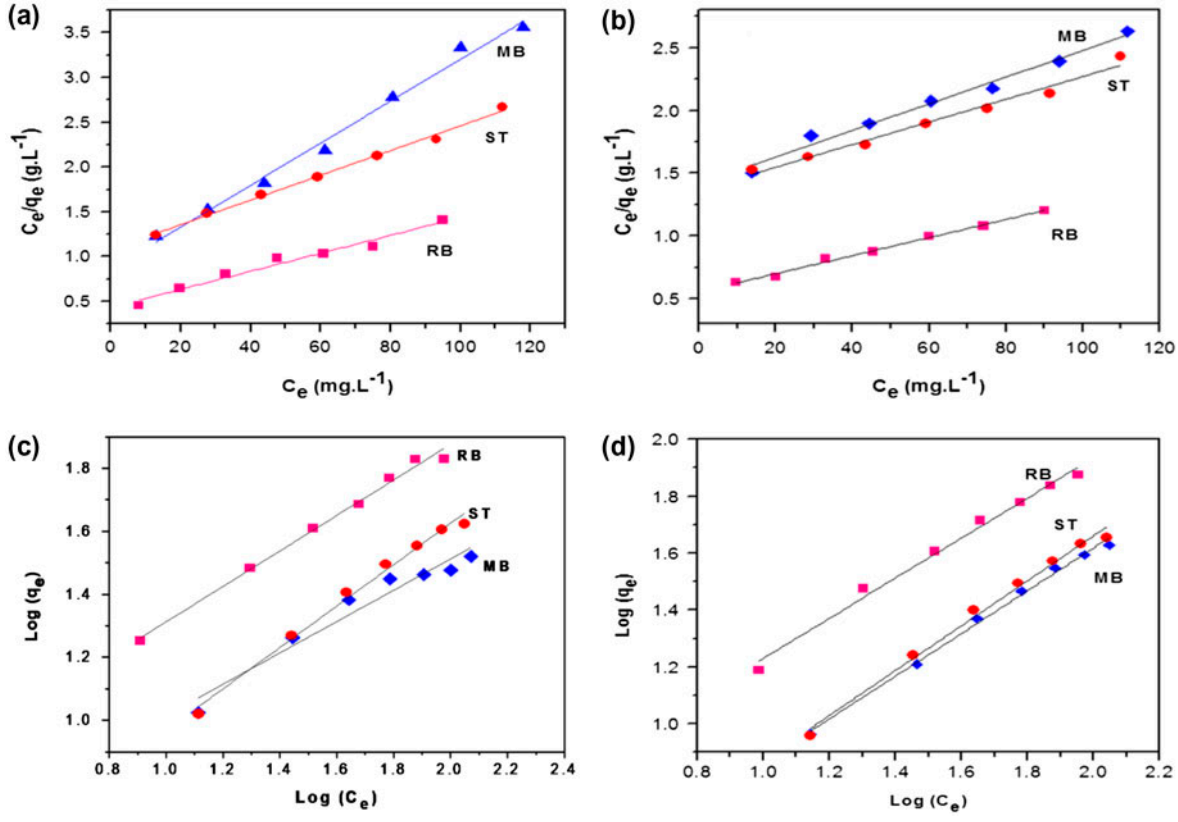

Fig. 9. Isotherms models for dyes adsorption; Langmuir (a) PAN, (b) EDA-g-PAN NFs and Freundlich (a) PAN (b) EDA-g-PAN NFs.

Table 3
Langmuir and Freundlich isotherms constants for the adsorption of dyes onto PAN and EDA-g-PAN NFs membranes

PAN				
Langmuir	Dye	q_{max}	K	r^2
	MB	42.662	0.027	0.989
	ST	72.465	0.013	0.995
	RB	99.305	0.023	0.967
Freundlich	Dye	K_f	n	r^2
	MB	3.293	2.011	0.941
	ST	5.979	1.522	0.988
	RB	5.609	1.775	0.990
EDA-g-PAN				
Langmuir	Dye	q_{max}	K	r^2
	MB	94.070	0.008	0.981
	ST	110.620	0.007	0.975
	RB	138.696	0.013	0.993
Freundlich	Dye	K_f	n	r^2
	MB	1.307	1.332	0.995
	ST	1.210	1.268	0.989
	RB	3.356	1.420	0.989

Fig. 9(a)–(d) shows the Langmuir (Fig. 9(a) and (b)) and Freundlich (Fig. 9(c) and (d)) isotherms plots. Both plot showed good fitting to the data, which suggests that along with monolayer formation some condensation/diffusion has also occurred. Table 3 shows the values of q_m and K (Langmuir), and n and K_f (Freundlich) calculated from the slope and intercept of the isotherms plots. q_m for RB, ST and MB onto EDA-g-PAN NFs membranes were much higher compare with most of the values reported in literature for these dyes [38]. The values of n suggests ($1 < n < 10$, favourable adsorption) favourable adsorption for all the dyes [39].

Furthermore, the favourability of the adsorption in case of Langmuir is determined in term of dimensionless constant separation factor or equilibrium parameter $R_{L,}$ calculated with Eq. (6):

$$R_L = \frac{1}{(1 + K_L C_0)} \tag{6}$$

where C_0 is the highest initial concentration of adsorbate (mg L^{-1}) and K_L (L mg^{-1}) is Langmuir constant.

R_L indicates the shape of the isotherm to be either unfavourable ($R_L > 1$), linear ($R_L = 1$), favourable ($0 < R_L < 1$) or irreversible ($R_L = 0$). The values for R_L between 0 and 1 (Table 4**)** confirms the favourability of adsorption.

Table 4
R_L values for the adsorption of dyes onto PAN and DETA-g-PAN NFs membranes

	RL		
Membrane	MB	RB	ST
PAN	0.21	0.24	0.36
EDA-g-PAN	0.49	0.354	0.52

4. Conclusion

EDA-g-PAN NFs membrane was prepared via electrospinning and chemical grafting techniques. Grafting (64%) with no change in the physical nature and colour was confirmed by FT-IR spectra. The adsorption kinetic followed pseudo-second-order model and intraparticle diffusion was not the only rate-limiting step. The adsorption data for the dyes fitted well to Langmuir and Freundlich equations. The order of adsorption capacity (q_{max}) obtained from Langmuir plot was: MB (94.07 mg/g) < ST (110.62 mg/g) < RB (138.69 mg/g). These values are more than most of the values reported in literature.

Acknowledgement

The Authors extend their appreciation to the Deanship of Scientific Research at King Saud University for funding the work through the research group project no. RGP-VPP-311.

References

[1] S. Haider, Y. Khan, W. Al-masry, A. Haider, Z. Ullah, R. Ullah, Electrospun Nanofibers and Their Functionalization. Nova Publishers Inc., New York, NY, 2013, pp. 75–92.
[2] K. Saeed, S. Haider, T.-J. Oh, S.-Y. Park, Preparation of amidoxime-modified polyacrylonitrile (PAN-oxime) nanofibers and their applications to metal ions adsorption, J. Membr. Sci. 322 (2008) 400–405.
[3] B.S.P. Ratna, Pollution due to synthetic dyes toxicity & carcinogenicity studies and remediation, Int. J. Environ. Sci. 3 (2012) 940–955.
[4] J. Mittal, D. Jhare, H. Vardhan, A. Mittal, Utilization of bottom ash as a low-cost sorbent for the removal and recovery of a toxic halogen containing dye eosin yellow, Desalin. Water Treat. (2013) 1–12. doi:10.1080/19443994.2013.803265.
[5] A. Mittal, R. Jain, J. Mittal, M. Shrivastava, Adsorptive removal of hazardous dye quinoline yellow from waste water using coconut-husk as potential adsorbent, Fresen. Environ. Bull. 19 (2010) 1–9.
[6] V.K. Gupta, A. Mittal, D. Jhare, J. Mittal, Batch and bulk removal of hazardous colouring agent rose bengal by adsorption techniques using bottom ash as adsorbent, R. Soc. Chem. Adv. 2 (2012) 8381–8389.
[7] A. Mittal, Adsorption kinetics of removal of a toxic dye, malachite green, from wastewater by using hen feathers, J. Hazard. Mater. 133 (2006) 196–202.
[8] A. Mittal, D. Jhare, J. Mittal, Adsorption of hazardous dye eosin yellow from aqueous solution onto waste material de-oiled soya: Isotherm, kinetics and bulk removal, J. Mol. Liq. 179 (2013) 133–140.
[9] H. Daraei, A. Mittal, M. Noorisepehr, F. Daraei, Kinetic and equilibrium studies of adsorptive removal of phenol onto eggshell waste, Environ. Sci. Pollut. Res. 20 (2013) 4603–4611.
[10] A. Mittal, V. Thakur, J. Mittal, H. Vardhan, Process development for the removal of hazardous anionic azo dye congo red from wastewater by using hen feather as potential adsorbent, Desalin. Water Treat. 52 (2013) 227–237.
[11] A. Mittal, J. Mitta, L. Kurup, Utilization of hen feathers for the adsorption of indigo carmine from simulated effluents, J. Environ. Prot. Sci. 1 (2007) 92–100.
[12] A. Mittal, Removal of the dye, amaranth from wastewater using hen feathers as potential adsorbent, Electron J. Environ. Agric. Food Chem. 5 (2006) 1296–1305.
[13] J. Mittal, V. Thakur, A. Mittal, Batch removal of hazardous azo dye Bismark Brown R using waste material hen feather, Ecol. Eng. 60 (2013) 249–253.
[14] A. Mittal, Use of hen feathers as potential adsorbent for the removal of a hazardous dye, brilliant blue FCF, from wastewater, J. Hazard. Mater. 128 (2006) 233–239.
[15] S. Haider, N. Bukhari, S.Y. Park, Y. Iqbal, W.A. Al-Masry, Adsorption of bromo-phenol blue from an aqueous solution onto thermally modified granular charcoal, Chem. Eng. Res. Des. 89 (2011) 23–28.
[16] R. Sanghi, B. Bhattacharya, Review on decolorisation of aqueous dye solutions by low cost adsorbents, Color. Technol. 118 (2002) 256–269.
[17] J.P. Chen, L. Hong, S. Wu, L. Wang, Elucidation of interactions between metal ions and Ca alginate-based ion-exchange resin by spectroscopic analysis and modeling simulation, Langmuir 18 (2002) 9413–9421.
[18] L. Jin, Mechanisms of lead adsorption on chitosan/PVA hydrogel beads, Langmuir 18 (2002) 9765–9770.
[19] R. Coşkun, M. Yiğitoğlu, M. Saçak, Adsorption behavior of copper(II) ion from aqueous solution on methacrylic acid-grafted poly(ethylene terephthalate) fibers, J. Appl. Polym. Sci. 75 (2000) 766–772.
[20] S. Lacour, J.-C. Bollinger, B. Serpaud, P. Chantron, R. Arcos, Removal of heavy metals in industrial wastewaters by ion-exchanger grafted textiles, Anal. Chim. Acta 428 (2001) 121–132.
[21] C.A. Borgo, Y. Gushikem, Zirconium phosphate dispersed on a cellulose fiber surface: Preparation, characterization, and selective adsorption of Li+, Na+, and K+ from aqueous solution, J. Colloid Interface Sci. 246 (2002) 343–347.
[22] R. Liu, Y. Li, H. Tang, Synthesis and characteristics of chelating fibers containing imidazoline group or thioamide group, J. Appl. Polym. Sci. 83 (2002) 1608–1616.
[23] F. Sebesta, J. John, A. Motl, K. Stamberg, Evaluation of polyacrylonitrile (PAN) as a binding polymer for absorbers used to treat liquid radioactive wastes, Other Information: PBD: Nov 1995, Ed., 50 p.
[24] N. Arsalani, M. Hosseinzadeh, Synthesis and characterization of edta functionalized polyacrylonitriles and their metal complexes Iran, Polymer 14 (2005) 345–352.
[25] P. Sundaramoorthy, V.R.G. Dev, M.R. Devi, Physical and thermal properties of nano lead oxide loaded electrospun PAN nanofibres, Indian J. fibre Text. Res. 37 (2012) 16–19.
[26] S.R.R. Eslami Farsani, A. Shokuhfar, A. Sedghi, FT-IR study of stabilized pan fibers for fabrication of carbon fibers, World Acad. Sci. Eng. Technol. 50 (2009) 430–433.
[27] X.G. Wang, J.C.C. Chan, Y.H. Tseng, S.F. Cheng, Synthesis, characterization and catalytic activity of ordered SBA-15 materials containing high loading of diamine functional groups, Microporous Mesoporous Mater. 95 (2006) 57–65.
[28] S. Halabhavi, S. Asha, P. Parameswar, R. Somashekar, S. Ganesh, Interaction of 8 MeV electron beam with P31 bombyx mori silk fibers, Mater. Sci. Appl. 2 (2011) 827–832.
[29] N. Bilba, D. Bilba, G. Moroi, Synthesis of a polyacrylamidoxime chelating fiber and its efficiency in the retention of palladium ions, J. Appl. Polym. Sci, 92 (2004) 3730–3735.
[30] S. Ata, M.I. Imran Din, A. Rasool, I. Qasim, I. Ul Mohsin, Equilibrium, thermodynamics, and kinetic sorption studies for the removal of coomassie brilliant blue on wheat bran as a low-cost adsorbent, J. Anal. Method. Chem. 2012 (2012) 1–8.

[31] P.S. Kumar, K. Kirthika, Equilibrium and kinetic study of adsorption of nickel from aqueous solution onto vael tree leaf powder, J. Eng. Sci. Technol. 4 (2009) 351–363.
[32] H. Qiu, L. Lv, B.-C. Pan, Q.-J. Zhang, W.-M. Zhang, Q.-X. Zhang, Critical review in adsorption kinetic models, J. Zhejiang Univ. Sci. A 10 (2009) 716–724.
[33] N.A. Oladoja, C.O. Aboluwoe, Y.B. Oladimeji, Kinetics and isotherm studies on methylene blue adsorption onto ground palm kernel coat, Turkish J. Eng. Environ. Sci. 32 (2008) 303–312.
[34] J.P. Chen, S.N. Wu, K.H. Chong, Surface modification of a granular activated carbon by citric acid for enhancement of copper adsorption, Carbon 41 (2003) 1979–1986.
[35] W.J. Weber, J.C. Morris, Kinetics of adsorption on carbon from solution, J. Sanit. Eng. Div. Am. Soc. Civ. Eng. 89 (1963) 31–60.
[36] I.D. Mall, V.C. Srivastava, N.K. Agarwal, I.M. Mishra, Removal of congo red from aqueous solution by bagasse fly ash and activated carbon: Kinetic study and equilibrium isotherm analyses, Chemosphere 61 (2005) 492–501.
[37] I.D. Mall, V.C. Srivastava, N.K. Agarwal, Removal of orange-G and methyl violet dyes by adsorption onto bagasse fly ash—kinetic study and equilibrium isotherm analyses, Dyes Pigm. 69 (2006) 210–223.
[38] S. Haider, F. Binagag, A. Haider, W.A. Al-Masry, Electrospun oxime-grafted-polyacrylonitrile nanofiber membrane and its application to the adsorption of dyes, J. Polym. Res. 21 (2014) 1–13.
[39] K. Kadirvelu, C. Namasivayam, Agricutural by-product as metal adsorbent: Sorption of lead(II) from aqueous solution onto coirpith carbon, Environ. Technol. 21 (2000) 1091–1097.